

CASC: Context-Aware Segmentation and Clustering for Motif Discovery in Noisy Time Series Data

Saachi Jain, David Hallac, Rok Susic, Jure Leskovec

Stanford University
 {saachi,hallac,rok,jure}@stanford.edu

Abstract

Complex systems, such as airplanes, cars, or financial markets, produce multivariate time series data consisting of system observations over a period of time. Such data can be interpreted as a sequence of *segments*, where each segment is associated with a certain *state* of the system. An important problem in this domain is to identify repeated sequences of states, known as *motifs*. Such motifs correspond to complex behaviors that capture common sequences of state transitions. For example, a motif of “making a turn” might manifest in sensor data as a sequence of states: slowing down, turning the wheel, and then speeding back up. However, discovering these motifs is challenging, because the individual states are unknown and need to be learned from the noisy time series. Simultaneously, the time series also needs to be precisely segmented and each segment needs to be associated with a state. Here we develop *context-aware segmentation and clustering* (CASC), a method for discovering common motifs in time series data. We formulate the problem of motif discovery as a large optimization problem, which we then solve using a greedy alternating minimization-based approach. CASC performs well in the presence of noise in the input data and is scalable to very large datasets. Furthermore, CASC leverages common motifs to more robustly segment the time series and assign segments to states. Experiments on synthetic data show that CASC outperforms state-of-the-art baselines by up to 38.2%, and two case studies demonstrate how our approach discovers insightful motifs in real-world time series data.

1 Introduction

Multivariate time series datasets represent the state of a system via a sequence of sensor readings. Directly extracting meaningful insights from time series data is challenging, since the relationships between readings are often complex and mutated by noise. Not all sensors are important all the time, and key information may lie in the connection between readings across different timestamps rather than within individual observations themselves. To understand this complex data, it is useful to distill the time series into a sequence of *segments*, where each segment represents an interval of time that is characterized by a specific *state*. Each state is thus an interpretable template for system behavior which can repeat itself many times across the time series.

These segments do not appear in isolation; the context in which a segment occurs provides critical insights and can be

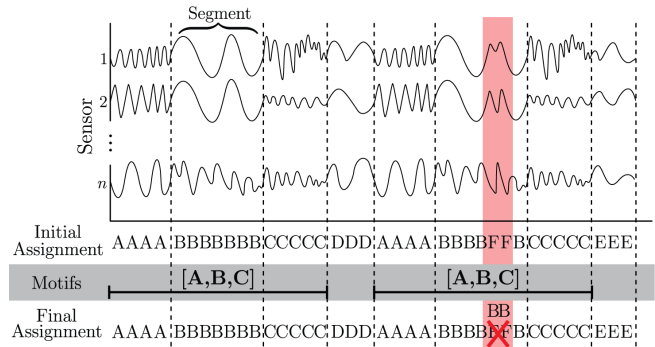


Figure 1: CASC partitions the time series, assigning each segment to a state (A , B , etc.). CASC further discovers motifs (repeated sequences of states), using them to improve segmentation in the presence of noise. Here, the motif is used to correct the updated states on the right.

just as useful as the state itself. It is therefore important to discover *motifs*, which represent a sequence of state transitions. In a car, a single segment may indicate that the driver is slowing down, but the sequence of slowing down, turning the wheel, and then speeding up implies that the vehicle is in a motif known as a “turn”. A motif is then an abstraction over multiple segments in the time series. It does not specify how long a driver slows down before turning, but only that deceleration occurred. Motifs formalize repeated patterns of states, even when the underlying segments for those states have variable durations. Once learned, these motifs can be used to improve one’s estimates of the states themselves. This context-aware motif-based assignment is especially useful for adjusting to noise in the data. For example, if a noisy segment is (incorrectly) assigned to the wrong state, yet the sequence it is in is “close to” being an instance of a known motif, one can use this motif to re-assign the segment to the correct state (Figure 1).

Discovering motifs in temporal datasets requires an unsupervised way of locating and labeling repeated behaviors. In general, as the states themselves are unknown, methods must simultaneously uncover the states, segment the time series, assign segments to states, and then identify the repeated motifs. Unlike standard time series segmentation techniques (Hallac, Nystrup, and Boyd 2016; Himberg et al. 2001), the states defining motifs can repeat themselves many

times across the time series. In contrast to clustering-only methods for state detection (Hallac et al. 2017; Smyth 1997; Keogh and Pazzani 2000), many segments can be assigned to the same state. Additionally, existing model-based approaches for motif discovery treat motifs as a final step and do not allow such motifs to influence and improve the robustness of the time series segmentation (Lin et al. 2007).

Here we introduce *Context-Aware Segmentation and Clustering* (CASC), a method for discovering motifs in time series data. Given a multivariate time series, CASC segments the dataset, where each segment belongs to one of K unique states. Simultaneously, CASC discovers a set of motifs, which can then be used to more robustly segment the time series. We formulate a large optimization problem over two model parameters: the first partitions the time series and assigns each segment to a state, and the second learns a set of motif templates over the states and identifies specific instances of each motif. Since these variables are combinatorial and coupled together in a highly non-convex manner, we heuristically solve the CASC optimization problem using alternating minimization. Iteratively, we cycle between using the existing segmentation scheme to identify states and greedily discover motifs, and then using the existing motifs to re-segment the time series in a context-aware manner. For both steps, we develop novel techniques to solve the sub-problems in an accurate and scalable way.

We evaluate CASC on several synthetic and real-world datasets. First, we analyze how accurately CASC is able to label the time series with known ground-truth states. We compare our method with several state-of-the-art baselines, showing that CASC outperforms the best of the baselines by up to 38.2%. Then, we evaluate CASC’s performance on discovering the ground-truth motifs. We also examine how robust CASC is to the presence of noisy data, measuring how performance fluctuates with varying amounts of noise.

Finally, we perform two real-world case studies by applying CASC to sensor data from both aircrafts and automobiles. We show that CASC discovers interesting and interpretable motifs that occur in flight and driving sessions.

Further Related Work. Recent approaches to time series segmentation often use distance-based metrics to identify different states (Keogh and Pazzani 2000). Additionally, they apply dimensionality reduction (Lin et al. 2007; Lin et al. 2003) or rule based approaches (Das et al. 1998; Li, Lin, and Oates 2012) to identify symbolic representations. However, distance-based methods have been shown to be unreliable in certain cases (Keogh and Lin 2005), and lose the interpretability of multivariate data-points. Model-based methods, such as TICC (Hallac et al. 2017), ARMA (Xiong and Yeung 2004), Gaussian Mixture Models (Banfield and Raftery 1993), and Hidden Markov Models (Smyth 1997), represent states as clusters using probabilistic models, and often can more accurately encode the relationships between sensors and the true underlying states.

Motif discovery is a common problem in time series data analysis (Chiu, Keogh, and Lonardi 2003). Methods for finding motifs include random projection (Buhler and Tompa 2002) and suffix arrays (Sahli, Mansour, and Kalnis 2014). Most of these methods assume motifs of fixed length. Some

methods also use distance metrics (Yankov et al. 2007). The problem of finding repeated patterns also appears in the field of computational genomics. ACME uses a combinatorial approach to find super-maximal motifs in DNA (Sahli, Mansour, and Kalnis 2014). Other bioinformatics models use edit-distance approaches to find motifs that vary slightly in appearance over the course of the sequence (Pal, Xiao, and Rajasekaran 2016). CASC departs from these methods in two respects. Firstly, CASC allows segments within a motif to have variable length while maintaining a given state. Moreover, unlike uniform scaling approaches (Yankov et al. 2007), CASC allows each state within a motif to scale independently. Secondly, CASC iterates by using the motifs to re-segment the original time series, encouraging noisy sequences that are similar to a motif to follow the motif template. This iteration allows for stronger motifs and more robust time series segmentation.

2 Problem Overview

Our input is defined as a sequence of T observations, $\mathbf{X} = X_1, X_2, \dots, X_T$, where each $X_i \in \mathbb{R}^N$ is the i -th observation in time and consists of N dimensions/features. As output, CASC aggregates consecutive sequences of observations and assigns them into one of K distinct states, also known as clusters. Consecutive observations that belong to a common state are known as a *segment*. Each segment is defined by a start time (b), end time (e), and state (k). Thus, $S_i = (b_i, e_i, k_i)$ implies that every observation between X_{b_i} and $X_{e_i - 1}$ is assigned to state k_i . The segments can then be combined into $\mathbf{S} = [S_1, \dots, S_{|\mathbf{S}|}]$, where:

1. The start time of S_1 is 1, and the end time of $S_{|\mathbf{S}|}$ is $T+1$.
2. $\forall i$, S_i ’s end time must equal S_{i+1} ’s start time.
3. $\forall i$, S_i and S_{i+1} must be assigned to different states.

From \mathbf{S} , we can derive a symbolic representation of the state sequence, as displayed in Figure 1. For notational convenience, we define \mathbf{U} as the list of states $[k_1, k_2, \dots, k_{|\mathbf{S}|}]$ assigned to segments $S_1, \dots, S_{|\mathbf{S}|}$.

While the states themselves are very useful, the order in which they appear represents a higher level of abstraction than the states alone. We define a *motif* as a template over segments, formalized by a sequence of states, i.e. $A \rightarrow B \rightarrow C$ for $k_i = A, k_{i+1} = B, k_{i+2} = C$, that commonly appears in the data. We let $\mathbf{M} = [(m_1, q^{(1)}), (m_2, q^{(2)}), \dots, (m_{|\mathbf{M}|}, q^{(|\mathbf{M}|)})]$ denote the list of motifs that appear in \mathbf{X} . Here, m_i is the ordered sequence of states that defines motif i , for example $[A, B, C]$. The other term in the tuple, $q^{(i)} = [q_1^{(i)}, \dots, q_{|q_i|}^{(i)}]$ is a list of instances of this motif. Each $q_i^{(j)}$ is a specific instance, a list of size $|m_i|$ showing the exact segments S_i that conform to motif m_i . Thus, we seek to solve for \mathbf{S} , the segments and their assigned states, and \mathbf{M} , the motifs and their corresponding instances. We place the following constraints on \mathbf{M} :

1. Every motif must contain at least 3 segments: $|m_i| > 2$.
2. Every motif must occur at least L times in the dataset: $|q_i| \geq L, \forall i$ (for the rest of this paper, we set $L = 10$).
3. Each segment S_i can be assigned to at most one motif.

4. For a motif instance, the corresponding segments must conform to the state assignments defined by the motif m_i .

CASC Problem Setup. Overall, CASC seeks to solve for \mathbf{S} and \mathbf{M} by optimizing the following objective subject to the above constraints on \mathbf{S} and \mathbf{M} :

$$\max_{\mathbf{S}, \mathbf{M}} \sum_{s \in \mathbf{S}} \left(\ell(s) + \mathbb{1}\{s \notin \mathbf{M}\} |s| \log \gamma \right) + \sum_{(m, q) \in \mathbf{M}} \sum_{i=1}^{|q|} \Psi(m, q^{(i)}),$$

Here, ℓ is the likelihood of a segment belonging to a state and the parameter $0 \leq \gamma \leq 1$ defines how strict we are at “forcing” observations to follow a motif pattern. Lower values of γ indicate more aggressive motif interventions, where we strongly encourage as many segments as possible to be part of a motif, even if the motif is extremely unlikely to have generated the observed data. The term $\Psi(m, q^{(i)})$ is a scoring metric incorporating the strength of the motifs found in the dataset. We discuss this metric in more detail in Section 5.

Likelihood Term. $\ell(s) = \ell((b, e, k))$ defines how likely it was that the given segment (from X_b to X_e) was generated by state k . We note that CASC is agnostic to the specific likelihood model used. That is, any potential model that specifies this likelihood would be valid, which allows CASC to apply to diverse types of data, from heterogeneous exponential families (Park et al. 2017) to categorical distributions.

In this paper, though, we define the likelihood using the Toeplitz Inverse Covariance-based Clustering (TICC) model (Hallac et al. 2017). TICC defines each state k by a block Toeplitz Gaussian inverse covariance matrix $\Theta_k \in \mathbb{R}^{N \times N}$ and empirical mean $\mu_k \in \mathbb{R}^N$, as

$$\ell((b, e, k)) = \sum_{i=b}^e \ell \ell(X_i, k) - \lambda \|\Theta_k\|_1 - \beta, \quad (1)$$

where

$$\ell \ell(X_t, k) = -(X_t - \mu_k)^T \Theta_k (X_t - \mu_k) + \log \det \Theta_k. \quad (2)$$

Here, TICC uses the log likelihood (up to a constant and scale) of observation X_t being generated from a Gaussian distribution defined by parameter Θ_k . It then subtracts an ℓ_1 lasso penalty as regularization (Tibshirani 1996) (governed by $\lambda > 0$) and a constant β term. Throughout this paper, we select λ and β using Bayesian Information Criteria (BIC), as suggested by the authors in the TICC paper.

3 CASC Algorithm

The CASC problem formulation is non-convex, and thus it is not tractable to solve for a global optimum. However, we can heuristically solve this non-convex objective by alternately minimizing over two sub-objectives.

Step 1: Generate motif candidates (Section 4). We use \mathbf{S} to dynamically generate a set of candidate motifs.

Step 2: Assign and score motifs (Section 5). We assign observations to states in a motif (or to no motif at all). We use a hidden Markov model to identify possible instances for each motif candidate, and then greedily assign segments to motifs while maintaining the restrictions described in Section 2. We then optimize \mathbf{S} based purely on the likelihood

term: if \mathbf{S} does not change, then we have reached convergence. Otherwise, we feed the optimized \mathbf{S} back to Step 1.

Once converged, we return \mathbf{S} and \mathbf{M} . We further can rank the output motifs in \mathbf{M} , showing the “strength” of each motif, using their final motif score. The scoring mechanism is described in Section 5.

4 Step 1: Motif Candidate Generation

Given our segmentation \mathbf{S} , we seek to find a candidate set of potential motifs. This initial candidate generation operates solely on the symbolic representation \mathbf{U} of \mathbf{S} ; we incorporate the likelihoods of individual segments during the re-assignment step in Section 5. We generate candidates in two phases: we find repeated patterns in \mathbf{U} , and then we filter these patterns to output a candidate set.

Step 1.1: Identify repeated patterns. We first find all maximal repeated subsequences that appear in \mathbf{U} using a suffix array (py-rstr max 2011). A maximal pattern is defined as a sequence that cannot be extended to either the left or right without changing the set of occurrences in \mathbf{U} (Sahli, Mansour, and Kalnis 2014). We require that each repeated pattern has at least L non-overlapping instances in \mathbf{U} .

Step 1.2: Select a motif candidate set. We next seek to select relevant patterns to form a motif candidate set. We cannot simply filter the patterns by frequency because an ideal motif candidate should also be a novel addition to the set. We design a dynamic way to filter motifs/patterns by assessing each new pattern against a null hypothesis that has the knowledge of all previously accepted candidate motifs.

For any pattern (candidate motif) p , let N_p be the number of non-overlapping occurrences of p in \mathbf{U} . Each pattern p produced via the suffix array can be represented as a sequence of components, where each component p_i is a state occurring individually with probability $\Pr(p_i)$ according to its empirical frequency in \mathbf{U} .

Assuming a model where each component appears independently, then the null hypothesis for the probability of observing the full pattern p is $\Pr(p) = \prod_i \Pr(p_i)$. The p-value of p is then the probability of at least N_p occurrences of p appearing according to our null hypothesis under a binomial model (Castro and Azevedo 2011). Let \mathcal{D} be a set of patterns that the null hypothesis already knows about. Initially, we set the null hypothesis to automatically know about the frequencies of individual states as well as any repeats of size 2 that occurred in \mathbf{U} . Then we define \mathcal{D} as:

$$\mathcal{D} = \{p \in [1, K]^2 \mid N_p \geq 2\} \cup \{k \in [1, K]\}. \quad (3)$$

Any pattern p in \mathcal{D} can be represented as a single component $\phi(p)$ with probability equal to the empirical probability of p :

$$\Pr(\phi(p)) = N_p / |\mathbf{U}|.$$

We sort \mathcal{D} by decreasing length, breaking ties by decreasing empirical probability. \mathcal{D} thus acts as a “reference set” of subsequences. For any pattern p , we can construct a new pattern $f(p, \mathcal{D})$: for every $p' \in \mathcal{D}$ in sorted order, replace all non-overlapping instances of p' in p with $\phi(p')$. Then, after initializing \mathcal{D} as in Equation 3, we sort all patterns in order of increasing length. For each pattern p , if

$$\Pr \left(\mathcal{B}(|\mathbf{U}|, \Pr(f(p, \mathcal{D}))) \geq C(p, \mathbf{U}) \right) \leq \alpha$$

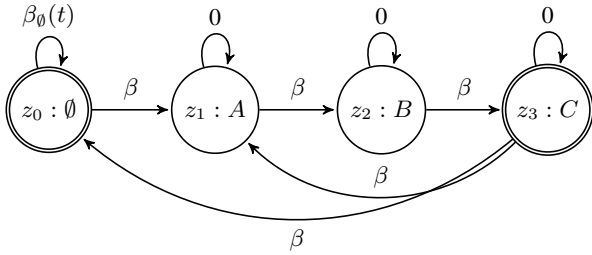


Figure 2: HMM for a motif $[A, B, C]$. Edges represent transition costs. z_1, z_2, z_3 are motif states, while z_0 is a garbage state representing observations that are not part of a motif.

for some threshold α , accept p as a motif candidate. We then add p to \mathcal{D} for evaluation of the next pattern.

5 Step 2: Motif Assignment and Scoring

We now re-assign observations according to this candidate motif set. This step proceeds in four phases:

Step 2.1: Identify instances of each motif. We identify instances of a motif by assigning observations/segments into states that are a part of a given motif. To this end, we define a time-varying hidden Markov model to model the entire sequence of observations \mathbf{X} . Figure 2 shows an example of our HMM for motif $A \rightarrow B \rightarrow C$. For a motif candidate m , the HMM has a hidden state z_i for each CASC segment $m_i \in m$. Our emission probabilities for these motif states are governed by the TICC log likelihood described in Equation 2, such that $\log \Pr(X_i | z_j) = \ell\ell(X_i, m_j)$.

We create a “garbage” state z_0 which signifies that the observation is not in the motif (Ge and Smyth 2000). This allows the HMM to ignore irrelevant observations. Let X_i ’s original assignment according to \mathbf{S} be defined as u_i . We then formalize z_0 as u_i , discounted by the non-motif penalty $\gamma < 1$. The emission probability for X_i from the garbage state is then $\log \Pr(X_i | z_0) = \ell\ell(X_i, u_i) + \log(\gamma)$.

CASC prioritizes assignments to motifs even if a different assignment is more likely. γ encapsulates how much less likely the motif can be while still being picked over the “most likely” sequence. A $\gamma = 1$ would not assign any motifs, since the garbage state represents an optimal sequence. A lower γ such as $\gamma = 0.6$ will be more aggressive, exploring motifs even when the likelihood might decrease.

Motif stages can transition only to themselves or into the next motif stage: in Figure 2, z_1 can change state to z_2 with penalty β , the TICC switching penalty. However, z_1 cannot transition to state z_3 . The garbage state can switch into itself or start a motif by switching into z_1 ; however, once z_1 has been entered, the only way to return to garbage is by finishing the motif. The last state (z_3) can either start another motif by switching to z_1 or enter the garbage state z_0 .

States do not incur a switching penalty when switching to themselves. The notable exception is the garbage state, where we define the penalty in the garbage state using $\beta_0(t)$:

$$\beta_0(t) = \beta \mathbb{1}(t \neq 1 \wedge u_{t-1} \neq u_t)$$

$\beta_0(t)$ thus adds a cost of β when transitioning from z_0 to itself if, in \mathbf{S} , the observation incurred a switching penalty.

Both z_0 and the first motif state (in our example, z_1) are valid starting states. z_0 and the last motif state (z_3) are the only valid end states. With our HMM fully defined, we use the Viterbi algorithm, a dynamic programming method, to find the most likely sequence of states $\in \{z_0, \dots, z_{|m|}\}$ given the observations (Martin and Jurafsky 2009).

Step 2.2: Score motif instances. Since we built a separate HMM for each motif in Step 2.1, it is possible for a single observation to appear in multiple motifs, violating the restrictions in Section 2. Therefore, it is necessary to develop a way of ranking motif instances. Each instance has two factors influencing its significance: the importance of its motif itself and the individual likelihood of the observations.

Motif Score: Let N_m be the number of instances of m identified via the HMM. We again define our null model for a motif as the probability of each state m_i occurring independently. However, here the null model only encodes the initial empirical frequencies of individual states. Our null model for m is then: $\Pr(m) = \prod_i^{|m|} \Pr(m_i)$ where $\Pr(m_i)$ is computed from the frequency counts of the symbolic representation \mathbf{U} . According to the null model, the expected number of instances of m is $|\mathbf{U}| \Pr(m)$. We define the motif score as the G-score (Aggarwal and Han 2014):

$$\Upsilon(m) = 2N_m (\log N_m - \log |\mathbf{U}| \Pr(m)).$$

Instance Score: We now formalize the second component of our scoring metric, which evaluates an individual instance of a motif candidate. Let q_i be the i -th instance of the motif m . For each observation X_j belonging to a segment in q_i (for convenience, we denote this as $X_i \in q_i$), let $u_i^{(m)}$ be the state assigned to X_i by m ’s HMM and u_i be the state assigned according to \mathbf{S} . We then compute the instance score as the log ratio between the q_i ’s likelihood according to the HMM and the likelihood according to \mathbf{S} (Hughey and Krogh 1996):

$$\Delta(m, q_i) = \sum_{X_i \in q_i} 2(\ell\ell(u_i^{(m)}) - \ell\ell(u_i)).$$

Then the total score for a motif instance is:

$$\Psi(m, q) = \Upsilon(m) + \Delta(m, q_i).$$

Step 2.3: Greedy allocation of observations to motifs.

Having curated a set of motif instances in Step 2.1, we now need to allocate each observation X_t to either a single motif or no motif according to the constraints from Section 2.

After sorting the instances according to the above score, we greedily allocate motifs to observations using a system of locks and bids (Algorithm 1). After all motif instances have been processed, we only accept instances for motifs that are complete. This bid/lock scheme ensures that no X_i is claimed by multiple motif instances and that every accepted motif has at least L instances. Any observation that does not belong to an accepted motif instance is set to its original assignment in \mathbf{S} . We then reconstruct \mathbf{M} and \mathbf{S} from this greedy allocation.

Step 2.4 Optimize \mathbf{S} over likelihood. Finally, we optimize solely on \mathbf{S} according to the likelihood term in Equation 1, which also updates the model parameters for each state. We do this by performing a single iteration of TICC

Algorithm 1: Greedy Motif Assignment

```
1 Sort instances by  $\Psi$ ; initialize  $X_1, \dots, X_T$  unlocked;
2 foreach  $(q, m) \in \text{motif instances}$  do
3   if any  $X_i$  covered by  $q$  is locked then
4     reject  $q$  and continue;
5   if  $m$  is complete then
6     Lock all observations covered by  $q$ ;
7     Remove other bids on those observations;
8   else
9     Place bid on all observations covered by  $q$ ;
10    if # instances bid by  $m \geq L$  then
11      Mark  $m$  as complete;
12      Lock all of  $m$ 's current bids;
13      Remove other bids on those observations;
14 Retrieve motif instances that are permanently locked;
15 Construct and retrieve  $M$ ;
```

on the S returned by Step 2.3. TICC updates its state model according to the given segmentation, and returns a new S that optimizes the likelihood of the observations. If S does not change due to this step, CASC has converged.

6 Convergence and Runtime Complexity

CASC alternates between Step 1 and Step 2, feeding the S from Step 2.4 back into Step 1. CASC converges when optimizing S in Step 2.4 does not change the segmentation. The number of iterations that CASC needs to converge is dataset dependent, but typically is on the order of tens of iterations. The runtime of each step of CASC is as follows:

Step 1: Candidate generation. For a time series of length T and minimum motif length L , we identify at most T/L patterns from the suffix array. Let C be the number of eventually accepted motif candidates. Since construction of the suffix array takes linear time, generation of motif candidates takes worst case time $O((T/L)C + T)$. However, $C \ll T$ since motif construction occurs from the collapsed form U and is further constrained by the significance threshold α . We can optionally cap C by truncating the set according to p-score. This step thus takes linear time in T .

Step 2: Motif assignment and scoring. Assuming any motif candidate has at most r states, then the execution of Step 2.1 takes $O(rT)$ time due to the chain structure of the HMM. We can identify instances for each motif candidate in parallel. Scoring the instances in Step 2.2 thus takes constant time per motif instance. In the worst case for Algorithm 1, each motif has instances that cover all T observations. In such a scenario, each motif candidate can only bid on an observation once, so the algorithm can take worst case $O(CT)$. Practically, however, this is a loose upper bound since such a scenario would indicate an extremely redundant candidate set and would not pass through the filter in Step 1. Thus, this algorithm takes runtime linear in T . Finally, since TICC is also linear in T , Step 2 takes linear time, $O(T)$. In total, each iteration of CASC takes linear time in T , which we further verify experimentally in Section 7.

7 Evaluation

We performed an extensive evaluation of CASC’s performance on a range of scenarios and different parameter values. Specifically, we seek to measure CASC’s ability to identify common motifs in the presence of noise, as well as its accuracy in assigning points to the correct underlying states. For evaluations in this section, we use synthetic datasets, since they provide a known ground truth which we require for comparing CASC with state-of-the-art baseline methods. Later, in Section 8, we apply CASC to two real-world datasets. To run the experiments, we built a CASC solver that implements the algorithm described in Section 3¹. Given a multivariate time series dataset and the CASC parameter values, our solver returns the ranked motifs, the motif assignments, and the state assignments for each observation.

Dataset Generation. We generate our dataset using the same method as in the original TICC paper (Hallac et al. 2017). Our ground-truth synthetic time series has a total of 150,000 observation points, each point being in \mathbb{R}^5 . Points are taken from K states; we use $K = 10$ in our experiments. We first assign observation points to states and then generate specific observation values for each data point.

To create the assignment, we compose the time series from 1,000 “macro-segments”, each containing 150 points. Each macro-segment begins with 6 “garbage” segments of 15 points, where points within each segment are assigned randomly to one of K states. All points in one “garbage” segment are assigned the same state. These garbage segments are followed by 4 “motif” segments of 15 points each with states $A \rightarrow B \rightarrow C \rightarrow D$. Using these ground truth assignments, we form random ground truth covariances $\Sigma_1, \dots, \Sigma_K$ for each state through the method described in (Mohan et al. 2014). Each data-point from ground truth state k is then drawn from a multivariate normal distribution with zero mean and covariance Σ_k as in (Hallac et al. 2017).

We introduce noise into our segments as follows. For every segment, with probability ϵ , we perturb observations in that segment by a random non-motif state. For example, suppose a segment with a ground truth state i is set to be perturbed. We pick a random state $j \notin \{A, B, C, D\}$ (the non-motif states). Rather than using Σ_i to generate data, we draw from a distribution with covariance $0.7\Sigma_j + 0.3\Sigma_i$, such that the new segment appears as if from the random state.

Robustness to Noise. To evaluate the effectiveness of CASC in noisy data, we create multiple datasets using the above method, each with a different ϵ value. A larger value of ϵ indicates greater noise in the data, since more segments will be perturbed. We run CASC at $\gamma = 0.8$ (later in this section, we evaluate the sensitivity of our results to the selection of γ) against TICC and the following baseline models: a Gaussian Mixture Model (Banfield and Raftery 1993), K-means with Euclidean distance, and a Hidden markov model with Gaussian Emissions.

Figure 3 shows the results from measuring the accuracy of these models on the motif segments against the ground

¹Our CASC solver and all code from the experiments in this section are available for download at <https://github.com/snap-stanford/casc>.

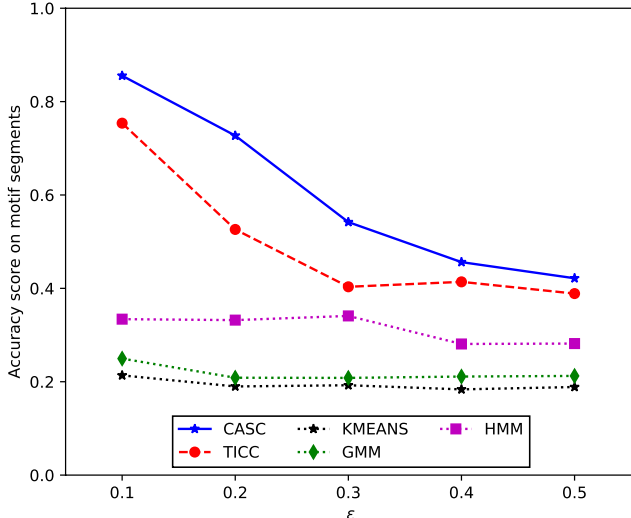


Figure 3: CASC and baseline accuracy scores on motif segments for synthetic data with varying levels of ϵ .

Table 1: Weighted F_1 scores on motif states A, B, C and D

ϵ	0.1	0.2	0.3	0.4	0.5
CASC	0.759	0.719	0.518	0.464	0.440
TICC	0.736	0.599	0.419	0.462	0.436
KMEANS	0.217	0.208	0.198	0.192	0.202
GMM	0.234	0.185	0.190	0.191	0.219
HMM	0.252	0.269	0.283	0.256	0.263

truth. The accuracy gives, for every point that was generated as part of a ground truth motif $A \rightarrow B \rightarrow C \rightarrow D$, the probability that this point was properly classified into the correct state. As shown, CASC classifies these segments with higher accuracy than any of the other baselines at all values of ϵ , outperforming TICC (the second-best performing method) by up to 38.2%. Interestingly, as ϵ rises initially up to about 0.3, CASC outperforms TICC by an increasing margin, which means that CASC is able to successfully utilize context information to correct state assignments. As expected, when ϵ rises even further, the support of $A \rightarrow B \rightarrow C \rightarrow D$ decreases, which limits CASC’s ability to identify it as a strong motif and to correct assignments missed by TICC. The gap between CASC and TICC thus narrows with higher levels of ϵ as CASC corrects fewer state assignments in the presence of increasing amounts of noise.

To absorb planted noise, CASC must adapt the parameter values of states A, B, C , and D , so that the noisy assignments are included. We seek to evaluate the impact of these adaptations over the entire dataset. In Table 1, we evaluate the F_1 scores for states A, B, C , and D over the full dataset, including times where they are assigned in the garbage segments. These scores are weighted by the support of these states within the ground truth dataset. CASC continues to significantly outperform TICC and other baselines, especially when the amount of noise is reasonable ($\epsilon < 0.4$). This shows how CASC can optimize accuracy on the motif segments while correctly ignoring the garbage segments.

Motif Identification. We further evaluate CASC’s accuracy in identifying the entire sequence $A \rightarrow B \rightarrow C \rightarrow D$ as

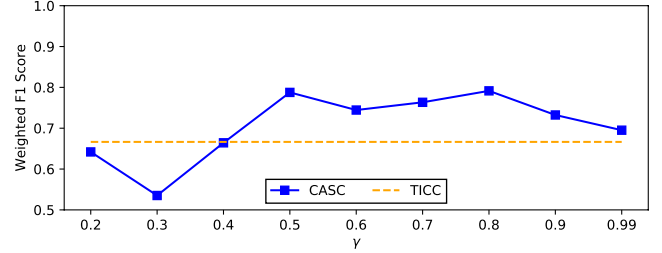


Figure 4: Weighted F_1 scores on motif states for varying γ . Here, all values of γ above 0.4 outperform TICC’s F_1 score.

a motif. We run CASC for $\epsilon = 0.2$, labeling each observation as 1 if it is included in the motif and 0 otherwise. The true labels thus assign each point as 0 unless it is part of the $A \rightarrow B \rightarrow C \rightarrow D$ sequence. For this experiment, CASC achieves an F_1 score of 0.79, showing that it successfully achieves the balance of properly labeling the true, but noisy, motifs, while not being overly aggressive and wrongly assigning incorrect sequences in the time series to the same motif. We note that the baseline methods are unable to perform this operation of recovering specific motifs, so there are no comparable results for their performance on this task.

γ -robustness. We evaluate robustness to the parameter γ , which encapsulates the aggressiveness of “forcing” observations to follow motifs. Smaller γ ’s encourage sequences to conform to known motif patterns, even if they are not a perfect fit. Higher values of γ only encourage motifs to exist when there is a near-perfect alignment. We run CASC with $\epsilon = 0.2$ and plot the weighted F_1 score on the motif states A, B, C , and D (including times where they are assigned to garbage segments, similar to Table 1) in Figure 4. We see that CASC is robust to the selection of γ , obtaining a weighted F_1 score of above 0.69, the score that TICC achieves, for all $0.4 < \gamma \leq 0.99$. Because the initial motif filtering step only permits the algorithm to pursue plausible motifs, even low values of γ (which are overly aggressive) perform reasonably well because there are very few “incorrect” motifs that the dataset can be wrongly assigned to.

Scalability. Since time series datasets can be extremely long, the number of observations T dominates the runtime of CASC. We empirically measure the per-iteration runtime of CASC on synthetic data with $\epsilon = 0.2$ for increasing numbers of observations. We find that the growth in runtime empirically increases linearly with respect to T , solving a dataset of 1.5 million points in 3,700 seconds.. Thus, CASC can scalably handle long time series datasets.

8 Case Studies

Here, we run CASC on two real-world examples, using automobile and aircraft sensor data to demonstrate how our approach can be applied to discover insightful motifs.

Automobile Sensor Data. We first evaluate our algorithm on a multivariate car sensor dataset, provided by a large automobile company. We observe the following 7 sensors collected every 0.1 seconds over an hour of driving data on real roads in Germany: brake pedal position, acceleration (X-direction), acceleration (Y-direction), steering wheel angle, speed, engine RPM, and gas pedal position.

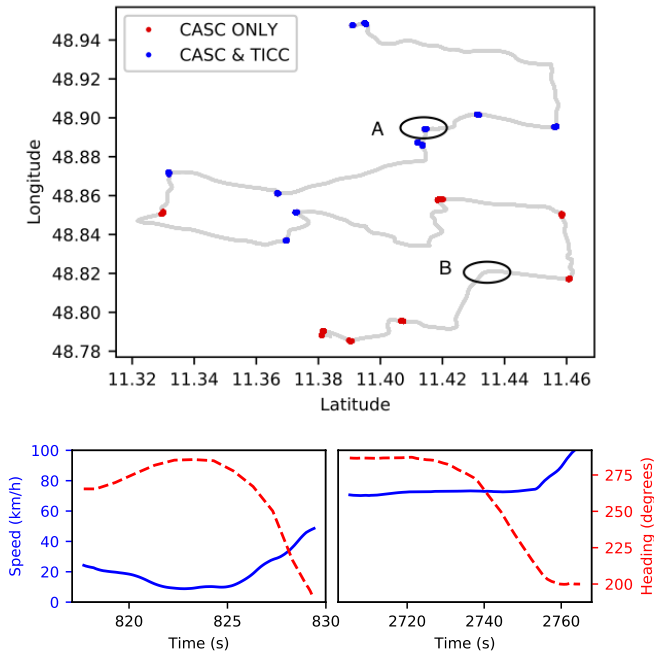


Figure 5: Top: Driver path over one session. Instances belonging to the “turn” motif are highlighted. Bottom: The speed/heading during Turn A (Left) and Turn B (Right).

We run CASC with 8 clusters on this dataset, and the results immediately identify a significant three stage motif that occurs 19 times during the one-hour session. After plotting the GPS coordinates of each sensor reading in Figure 5, we see that this motif corresponds to the driver turning the vehicle. Specifically, the three states appear to correspond to “slowing down”, “turning the wheel”, and “speeding up”. In TICC’s cluster assignment, only 11 of the 19 turns identified by CASC conformed to the motif pattern, and the turn pattern did not otherwise appear in TICC’s assignment. In these other cases, some noise in the sensor readings led TICC to assign one (or more) of the segments to an incorrect cluster. Thus, in an unsupervised way, CASC both identifies turns and clusters observations to make these turns more uniform.

There are some bends in the driving path which CASC does not identify as a turn. These are due to significant deviations in the template of a “typical turn” identified by the motif. Figure 5 depicts the speed and heading for the car during the section labeled A, which CASC identified as a turn. In this section, the car slows to 10 km/h during the turn before speeding back up. In contrast, during the turn B, the car maintained a speed of at least 70 km/h during the entirety of the turn. This stretch of road occurred on a highway, so even though the heading of the vehicle changed, this section of road did not conform to a classic three-stage “turn” motif, and thus was not classified as a turn by CASC.

CASC can thus identify directly interpretable segments of interest in an automobile dataset. Compared to state-of-the-art methods like TICC, CASC can intervene to more robustly cluster individual data points to make common behaviors, such as turns, appear uniform throughout the dataset in the presence of noise.

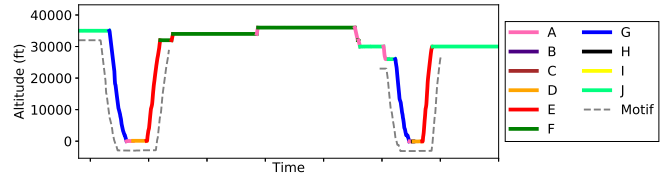


Figure 6: Airplane altitude over a 10 hour interval. The plot is colored according to its cluster segment, and the specific motif instances are underlined.

Airplane Sensor Data. We next analyze a dataset, provided by a large manufacturer, containing data from a single commercial aircraft over the course of several months. This multivariate dataset contained 1,459 sensors collected over 85 total flights, where data was sampled every 10 seconds. For computational scalability, we embed each 1,459-dimensional observation in a low-dimensional vector using principal component analysis. Here, we pick a value where the eigenvalues store 99% of the cumulative energy, which yields a vector in \mathbb{R}^{13} . We then run CASC with 10 clusters.

Labeling each cluster from A through J, CASC identifies the top motif as $J \rightarrow G \rightarrow A \rightarrow H \rightarrow D \rightarrow E$ (Figure 6). This motif is extremely consistent, occurring almost every time the plane lands for one flight then takes off for the next (since we do not care about the length of each segment, the layover time does not affect the presence of this motif). By analyzing the average sensor values across the motif instances, we find that the sensor values are extremely different across different clusters. By examining these readings, such as the ground speed and the change in altitude (in feet/minute), we can hand-label an interpretation for each stage of the identified motif as: (1) pre-descent, (2) descent, (3) taxiing, (4) boarding, (5) takeoff, and (6) ascent.

We note that CASC discovered this motif in a fully unsupervised manner. As shown, it was able to isolate an interesting repeated heterogeneous sequence of behaviors found across the time series. This has many practical benefits, as it can be used to auto-label the data with the different “stages” of a flight. Discovering motifs allows us to identify how these stages progress, and also lets us better label these stages when there is noise in the readings (due to turbulence, faulty sensors, or exogenous factors such as the weather).

9 Conclusion and Future Work

In this paper, we have developed a novel method for discovering motifs in time series data. Our approach, Context-Aware Segmentation and Clustering (CASC), leverages these motifs to better cluster time series data, discovering repeated segments and relevant trends. The promising results on both the synthetic experiments and case studies imply many potential directions for research. We leave for future work the analysis of CASC with different underlying clustering methods, rather than only TICC, the model we used in this paper. Furthermore, extending CASC to account for segment length, similar to hidden semi-Markov models, would open up this work to new applications and use cases.

References

- [Aggarwal and Han 2014] Aggarwal, C. C., and Han, J. 2014. *Frequent pattern mining*. Springer.
- [Banfield and Raftery 1993] Banfield, J. D., and Raftery, A. E. 1993. Model-based Gaussian and non-Gaussian clustering. *Biometrics* 803–821.
- [Buhler and Tompa 2002] Buhler, J., and Tompa, M. 2002. Finding motifs using random projections. *Journal of Computational Biology* 9(2):225–242.
- [Castro and Azevedo 2011] Castro, N., and Azevedo, P. J. 2011. Time series motifs statistical significance. In *Proceedings of the 2011 SIAM International Conference on Data Mining*, 687–698. SIAM.
- [Chiu, Keogh, and Lonardi 2003] Chiu, B.; Keogh, E.; and Lonardi, S. 2003. Probabilistic discovery of time series motifs. In *Proceedings of the ninth ACM SIGKDD international conference on Knowledge discovery and data mining*, 493–498. ACM.
- [Das et al. 1998] Das, G.; Lin, K.-I.; Mannila, H.; Renganathan, G.; and Smyth, P. 1998. Rule discovery from time series. In *KDD*, volume 98, 16–22.
- [Ge and Smyth 2000] Ge, X., and Smyth, P. 2000. Deformable Markov model templates for time-series pattern matching. In *Proceedings of the sixth ACM SIGKDD international conference on Knowledge discovery and data mining*, 81–90. ACM.
- [Hallac et al. 2017] Hallac, D.; Vare, S.; Boyd, S.; and Leskovec, J. 2017. Toeplitz inverse covariance-based clustering of multivariate time series data. In *Proceedings of the 23rd ACM SIGKDD International Conference on Knowledge Discovery and Data Mining*, 215–223. ACM.
- [Hallac, Nystrup, and Boyd 2016] Hallac, D.; Nystrup, P.; and Boyd, S. 2016. Greedy Gaussian segmentation of multivariate time series. *arXiv preprint arXiv:1610.07435*.
- [Himberg et al. 2001] Himberg, J.; Korpiaho, K.; Mannila, H.; Tikänmäki, J.; and Toivonen, H. T. 2001. Time series segmentation for context recognition in mobile devices. In *ICDM*.
- [Hughey and Krogh 1996] Hughey, R., and Krogh, A. 1996. Hidden Markov models for sequence analysis: extension and analysis of the basic method. *Bioinformatics* 12(2):95–107.
- [Keogh and Lin 2005] Keogh, E., and Lin, J. 2005. Clustering of time-series subsequences is meaningless: implications for previous and future research. *Knowledge and information systems* 8(2):154–177.
- [Keogh and Pazzani 2000] Keogh, E. J., and Pazzani, M. J. 2000. Scaling up dynamic time warping for datamining applications. In *Proceedings of the sixth ACM SIGKDD International Conference on Knowledge Discovery and Data Mining*, 285–289. ACM.
- [Li, Lin, and Oates 2012] Li, Y.; Lin, J.; and Oates, T. 2012. Visualizing variable-length time series motifs. In *Proceedings of the 2012 SIAM international conference on data mining*, 895–906. SIAM.
- [Lin et al. 2003] Lin, J.; Keogh, E.; Lonardi, S.; and Chiu, B. 2003. A symbolic representation of time series, with implications for streaming algorithms. In *Proceedings of the 8th ACM SIGMOD workshop on Research issues in data mining and knowledge discovery*, 2–11. ACM.
- [Lin et al. 2007] Lin, J.; Keogh, E.; Wei, L.; and Lonardi, S. 2007. Experiencing SAX: a novel symbolic representation of time series. *Data Mining and Knowledge Discovery* 15(2):107–144.
- [Martin and Jurafsky 2009] Martin, J. H., and Jurafsky, D. 2009. *Speech and language processing: An introduction to natural language processing, computational linguistics, and speech recognition*. Pearson/Prentice Hall.
- [Mohan et al. 2014] Mohan, K.; London, P.; Fazel, M.; Witten, D.; and Lee, S.-I. 2014. Node-based learning of multiple Gaussian graphical models. *The Journal of Machine Learning Research* 15(1):445–488.
- [Pal, Xiao, and Rajasekaran 2016] Pal, S.; Xiao, P.; and Rajasekaran, S. 2016. Efficient sequential and parallel algorithms for finding edit distance based motifs. *BMC genomics* 17(4):465.
- [Park et al. 2017] Park, Y.; Hallac, D.; Boyd, S.; and Leskovec, J. 2017. Learning the network structure of heterogeneous data via pairwise exponential Markov random fields. In *Artificial Intelligence and Statistics*, 1302–1310.
- [py-rstr max 2011] py-rstr max. 2011. Google code archive: py-rstr-max.
- [Sahli, Mansour, and Kalnis 2014] Sahli, M.; Mansour, E.; and Kalnis, P. 2014. ACME: A scalable parallel system for extracting frequent patterns from a very long sequence. *The VLDB Journal* 23(6):871–893.
- [Smyth 1997] Smyth, P. 1997. Clustering sequences with hidden Markov models. In *Advances in Neural Information Processing Systems (NIPS)*, 648–654.
- [Tibshirani 1996] Tibshirani, R. 1996. Regression shrinkage and selection via the lasso. *Journal of the Royal Statistical Society. Series B (Methodological)* 267–288.
- [Xiong and Yeung 2004] Xiong, Y., and Yeung, D.-Y. 2004. Time series clustering with ARMA mixtures. *Pattern Recognition* 37(8):1675–1689.
- [Yankov et al. 2007] Yankov, D.; Keogh, E.; Medina, J.; Chiu, B.; and Zordan, V. 2007. Detecting time series motifs under uniform scaling. In *Proceedings of the 13th ACM SIGKDD international conference on Knowledge discovery and data mining*, 844–853. ACM.